Mol. Cells *36*, 74-81, July 31, 2013
DOI/10.1007/s10059-013-0074-1
eISSN: 0219-1032

Molecules and Cells
http://molcells.org
Established in 1990

In-House Zinc SAD Phasing at Cu *K*α Edge

Min-Kyu Kim[1,5], Sangmin Lee[1,2,5], Young Jun An[1], Chang-Sook Jeong[1], Chang-Jun Ji[3], Jin-Won Lee[3], and Sun-Shin Cha[1,2,4,*]

***De novo* zinc single-wavelength anomalous dispersion (Zn-SAD) phasing has been demonstrated with the 1.9 Å resolution data of glucose isomerase and 2.6 Å resolution data of *Staphylococcus aureus* Fur (*Sa*Fur) collected using in-house Cu *K*α X-ray source. The successful in-house Zn-SAD phasing of glucose isomerase, based on the anomalous signals of both zinc ions introduced to crystals by soaking and native sulfur atoms, drove us to determine the structure of *Sa*Fur, a zinc-containing transcription factor, by Zn-SAD phasing using in-house X-ray source. The abundance of zinc-containing proteins in nature, the easy zinc derivatization of the protein surface, no need of synchrotron access, and the successful experimental phasing with the modest 2.6 Å resolution SAD data indicate that in-house Zn-SAD phasing can be widely applicable to structure determination.**

INTRODUCTION

Multi- or single-wavelength anomalous dispersion (MAD or SAD) methods are most commonly used for *de novo* phasing to solve protein structures with no proper homologous models. MAD is superior to SAD in that it allows the direct calculation of phase angles and has no phase-ambiguity issue (Hendrickson, 1991). Nevertheless, together with better data-collection facilities, cryogenic techniques, powerful programs for data processing, phasing, density modification (Wang, 1985) and automatic model building, SAD gets wide popularity due to its simplicity, fast data collection, and low radiation damage (Dauter et al., 2002).

SAD phasing has been reported at remote wavelengths above the absorption edge (Leonard et al., 2005) and even at Cu *K*α edge of in-house X-ray sources (Dauter et al., 2002; Debreczeni et al., 2003a; 2003b; 2003c; Evans and Bricogne, 2003; Roeser et al., 2005; Sarma and Karplus, 2006; Stevenson et al., 2004; Vennila and Velmurugan, 2011; Yogavel et al., 2007; 2009; 2010a; 2010b). The successful in-house SAD phasing opens new avenue of experimental phasing with in-house X-ray sources.

The presence of anomalous scatterers in protein crystals is prerequisite for SAD phasing. The most frequently used anomalous scatterers are introduced by recombinant DNA methods, as in selenomethionine (SeMet) substitution (Hendrickson et al., 1990) or by heavy-atom derivatization (e.g. Hg, Pt, lanthanides and actinides) (Blundell and Johnson, 1976; Boggon and Shapiro, 2000; Islam et al., 1998; Petsko, 1985; Rould, 1997). And metal ions inherently contained in metalloproteins (e.g. Zn, Fe or Cu) can also be used as anomalous scatterers. After the structure of crambin was solved by pioneering sulfur SAD (S-SAD) (Hendrickson and Teeter, 1981), native SAD has been explored to solve protein structures using lighter atoms such as sulfur from methionine or cysteine (Chayen et al., 2000; Debreczeni et al., 2003a; Mueller-Dieckmann et al., 2004; 2005; 2007; Olczak et al., 2003; Ramagopal et al., 2003a; Weiss et al., 2001), P atom in phosphate (Dauter and Adamiak, 2001), Cl atom from buffer (Dauter et al., 1999) as anomalous scatterers.

There are over 8 000 protein structures with zinc ions as ligands in the PDB, which shows that zinc ions are the most abundant metal ligand of proteins. Furthermore, about 5-10% of all proteins predicted from the genomes of all three domains of life are estimated to be zinc-containing proteins (Andreini et al., 2006). We have recently reported that multiple zinc ions can easily be charged onto the surface of proteins by using zinc-containing solutions and these surface-bound zinc ions are highly effective to determine protein structures by MAD/SAD phasing (Cha et al., 2012). The successful in-house S-SAD phasing cases (Debreczeni et al., 2003a; 2003b; 2003c; Lemke et al., 2002; Olsen et al., 2004; Pal et al., 2008; Sarma and Karplus, 2006; Yang and Pflugrath, 2001; Yogavel et al., 2010b), along with the fact that zinc has higher anomalous signal (f'' = 0.68 e^-) than sulfur (f'' = 0.56 e^-) at Cu *K*α edge, encouraged us to investigate the possibility of Zn-SAD phasing using in-house X-ray source. Here, we report two successful Zn-SAD phasing cases with the 1.9 Å resolution data of glucose isomerase (as a test case) and the 2.6 Å resolution data of *Sa*Fur (as a real case) both of which were collected using a MicroMax-007 HF rotating-anode X-ray generator.

[1]Marine Biotechnology Research Division, Korea Institute of Ocean Science and Technology, Ansan 426-744, Korea, [2]Ocean Science and Technology School, Pusan 606-791, Korea, [3]Department of Life Science and Institute for Natural Sciences, Hanyang University, Seoul 133-791, Korea, [4]Department of Marine Biotechnology, University of Science and Technology, Daejeon 305-333 Korea, [5]These authors contributed equally to this work.
*Correspondence: chajung@kiost.ac

Received February 28, 2013; revised April 9, 2013; accepted April 11, 2013; published online May 16, 2013

Keywords: anomalous scattering, experimental phasing, protein crystallography, SAD phasing, zinc

MATERIALS AND METHODS

Protein preparation and crystallization

Glucose isomerase

Glucose isomerase was purchased from Hampton Research (Lot No. 022004). According to the manufacturer's specifications, glucose isomerase was extensively dialyzed against 20 m*M* Tris-HCl pH 7.5 and subsequently diluted to a final concentration of 33 mg ml^{-1}. Crystals were obtained by the hanging-drop vapour-diffusion method at 295 K using a precipitant solution consisting of 0.2 M magnesium acetate, 0.1 M MES pH 6.5, 20% 2-methyl-2,4-pentanediol (MPD). Prior to the diffraction experiment, the crystals were soaked in same precipitant solution with 50 m*M* zinc acetate for 30 min - 2 h to introduce zinc ions into the protein surface.

SaFur

The *fur* gene (GenBank accession no. 15221618) was amplified by polymerase chain reaction using *S. aureus* genomic DNA as template. The gene was inserted downstream of the T7 promoter of the expression plasmid pET-11a(+) vector (Novagen, USA) and the resulting construct expressed residues 1-149 of the *Sa*Fur protein. After verifying the DNA sequence, plasmid DNA was transformed into *Escherichia coli* strain BL21 (DE3) pLysS (Promega Corp., USA). The cells were grown to OD_{600} of approximately 0.5 in Luria-Bertani medium (Merck) containing 50 μg ml^{-1} Ampicillin at 310 K and expression was induced by 1 mM isopropyl-β-D-1-thiogalactopyranoside (IPTG, Duchefa). After 4 h of induction at 310 K, the cells were harvested and resuspended in 20 mM Tris-HCl pH 8.0 containing 5% glycerol and 10 mM EDTA. The cells were disrupted by sonication and the cell debris was discarded by centrifugation at 20,000 × *g* for 30 min at 277 K. The resulting supernatant was loaded onto a 20 ml Heparin Sepharose™ column (GE Healthcare). The column was washed with a washing buffer consisting of 20 mM Tris-HCl pH 8.0, 5% glycerol, 10 mM EDTA and 50 mM NaCl. *Sa*Fur was eluted with the same buffer containing 300 mM NaCl. The partially purified protein fraction by Heparin Sepharose column was dialysed into washing buffer and loaded onto a column packed with 20 ml Q-Sepharose resin (GE Healthcare). This column was then washed with a gradient to 20 mM Tris-HCl pH 8.0, 5% glycerol, 10 mM EDTA and 1 M NaCl. The eluted fraction containing *Sa*Fur was concentrated and subsequently loaded onto a Superdex 75 HR 16/60 column (GE Healthcare), which was pre-equilibrated with a washing buffer. The *Sa*Fur protein was eluted at ~45 min with a flow rate of 1.5 ml min^{-1}. The purified *Sa*Fur was concentrated to approximately 15 mg ml^{-1} for crystallization. Crystals were grown at 295 K using the microbatch crystallization method. Small drops composed of 1 μl protein solution and an equal volume of a precipitant solution consisting of 30% (v/v) 1,2-propanediol, 0.1 M HEPES pH 7.5, 20% (v/v) PEG 400 were pipetted under a layer of a 1:1 mixture of silicon oil and paraffin oil in 72-well HLA plates (Nunc).

Data collection

A 1.9 Å resolution SAD data set for glucose isomerase and a 2.6 Å resolution SAD data set for *Sa*Fur were collected at wavelength of 1.54178 Å using a MicroMax-007 HF rotating-anode X-ray generator and an R-AXIS IV^{++} imaging-plate area detector (Rigaku, Japan) at the Korea Basic Science Institute, Republic of Korea. A total 720 frames of 1° oscillation were collected with the crystal-to-detector distance set to 150 mm in the case of glucose isomerase (Table 1) and a total 720 frames of 1° oscillation were collected with the crystal-to-detector distance set to 170 mm in the case of *Sa*Fur (Table 2).

Data processing and phasing

Diffraction data were processed and scaled using *DENZO* and *SCALEPACK* from the *HKL2000* program suite (Otwinowski and Minor, 1997). Experimental phasing was performed with the *AutoSol* program (Terwilliger et al., 2009) in the *PHENIX* suite (Adams et al., 2010) which is an experimental phasing pipeline that combines *HySS* (Hybrid Substructure Search) (Grosse-Kunstleve and Adams, 2003) for finding heavy-atom sites, *Phaser* (McCoy et al., 2007) or *SOLVE* (Terwilliger, 2002) for calculating experimental phases, and *RESOLVE* (Terwilliger, 2002) for density modification and model-building. The auto-built models from the phasing programs were completed using *COOT* (Emsley et al., 2010) and refinement was performed with a maximum-likelihood algorithm implemented in *CNS* (Brunger et al., 1998) or *REFMAC5* (Murshudov et al., 2011).

RESULTS AND DISCUSSION

A test case: structure determination of glucose isomerase using in-house Zn-SAD

Glucose isomerase is a highly suitable protein for testing different phasing methods based on the anomalous scattering of various metals because of the possibility of substituting its natural metal cofactors, Mn^{2+} or Mg^{2+}, with several other divalent metal ions (Ramagopal et al., 2003b). Thus, we selected glucose isomerase as a test protein to examine whether anomalous signal from zinc ions introduced by soaking can be used for in-house experimental phasing. A 1.9 Å resolution SAD data set (Table 1) was collected from a crystal that was cooled in a cryostream at 100 K after briefly being immersed in a cryoprotectant solution consisting of 20% MPD, 0.1 M MES pH 6.5, 0.2 M magnesium acetate and 50 m*M* zinc acetate dehydrate. The crystal of glucose isomerase belonged to the orthorhombic space group *I*222, with unit-cell parameters a = 92.927, b = 98.867, c = 102.638 Å. There was one molecule in the asymmetric unit, giving a Matthews coefficient (V_M) of 2.73 $Å^3$ Da^{-1} and a calculated solvent content of 54.92 % (Matthews, 1968).

Anomalous signals, which were evaluated by <*d''*/sig>, a good indicator of the strength of the anomalous signal, were over the threshold (0.80) (Sheldrick, 2010) to the highest resolution shell (Fig. 1A). The *AutoSol* program was used to find anomalous zinc substructures and produced a phase set with a figure of merit (FOM) before and after density modification of 0.42 and 0.90, respectively. The experimental electron-density map was clearly interpretable and a model with R_{work}/R_{free} of 0.1878/ 0.2084 was automatically built. The initial model was manually remodeled producing a final model with R_{work}/R_{free} of 0.1409/ 0.1625.

In fact, among the twelve heavy atom sites found by *HySS*, eight sites turned out to be the ordered sulfur positions from methionines or cysteines. Although the location of the relatively strong anomalous scatterers, zinc atoms (*f''* = 0.68), may facilitate the finding of sulfur atoms (*f''* = 0.56), the data evidently contained a meaningful anomalous scattering contribution originating from sulfur. This result is in accordance with the previous study that the location of Mn atoms facilitates the finding of sulfur atoms and the anomalous scattering of sulfur atoms contributes to SAD phasing (Ramagopal et al., 2003b).

Among four zinc ions finally modeled, two ions (Zn1 and Zn2) were located in the intrinsic metal binding sites and the other

Table 1. Data collection, phasing and refinement statistics

Protein name	Glucose Isomerase								
Data collection	SAD								
Space group	*I*222								
X-ray source	In-house Cu $K\alpha$								
Wavelength (Å)	1.54178								
Oscillation (°)	240	300	360	420	480	540	600	660	720
Unit cell parameters *a, b, c* (Å)	92.927, 98.867, 102.638								
Resolution (Å)[1]	50-1.9(1.93-1.9)								
Completeness (%)[1]	97.5(79.3)	97.6(80.5)	97.8(81.0)	97.8(80.8)	97.8(80.8)	97.8(80.9)	97.8(80.7)	97.8(80.7)	97.8(80.1)
R_{merge} (%)[1,2]	3.3(8.9)	3.3(8.8)	3.5(8.6)	3.4(8.6)	3.4(8.6)	3.5(8.6)	3.5(9.0)	3.6(9.0)	3.6(8.9)
$I/\sigma(I)$[1]	72.5(25.7)	80.6(29.0)	90.4(31.8)	97.3(17.7)	102.8(36.6)	109.7(38.3)	115.8(40.1)	121.2(42.6)	127.3(44.0)
Multiplicity	7.1(4.0)	9.0(5.0)	10.9(6.0)	12.7(7.0)	14.4(8.0)	16.2(8.9)	18.0(9.8)	19.9(10.9)	21.7(11.9)
Unique reflections	36,671	36,717	36,762	36,773	36,775	36,778	36,798	36,798	36,807
<*d*''/sig> of outer shell[3]	1.34	1.28	1.27	1.33	1.37	1.41	1.5	1.49	1.5
Phasing statistics									
Success of phasing	Failure	Success	Success	Success	Success	Success	Success	Success	Success
No. of Zn sites in initial model from *AutoSol*	9	11	11	12	12	12	13	13	14
Sites occupancies[6]	1.00	0.67-0.99	0.68-0.97	0.29-0.99	0.30-1.00	0.29-1.00	0.28-1.00	0.30-1.00	0.32-0.93
FOM[6]									
Before DM	0.21	0.43	0.46	0.47	0.47	0.48	0.49	0.49	0.42
After DM	0.81	0.78	0.78	0.78	0.78	0.78	0.78	0.78	0.90
Model-map CC[6]	0.06	0.57	0.69	0.70	0.71	0.69	0.71	0.70	0.83
R_{work}[4](R_{free}) (%)	0.5535/ 0.5579	0.2419/ 0.2687	0.2049/ 0.2296	0.1926/ 0.2200	0.2001/ 0.2340	0.2278/ 0.2597	0.2162/ 0.2426	0.2125/ 0.2408	0.1878/ 0.2084
Refinement statistics									
Resolution range (Å)	28.28-1.9								
No. reflections	34,963								
No. atoms									
Protein	3,044								
MPD	2								
Zinc ion	4								
Acetate	2								
Water	446								
R_{work}[4](R_{free}) (%)	14.09 (16.25)								
R.m.s. deviations[5]									
Bonds length (Å)	0.005								
Bond Angles (°)	1.093								

[1]The number in parentheses is for the outer shell.
[2]$R_{merge} = \Sigma_{hkl}\Sigma_i|I_i(hkl) - \langle I(hkl)\rangle|/\Sigma_{hkl}\Sigma_i I_i(hkl)$, where $I_i(hkl)$ is the intensity of observed reflection *hkl* and $\langle I(hkl)\rangle$ is the mean intensity of symmetry-equivalent reflections
[3]Data from *SHELXC* (Sheldrick, 2010)
[4]$R_{work} = \Sigma\,|F_o - F_c| \,/\, \Sigma\, F_o$
R_{free} was calculated with 5% of the reflections.
[5]R.m.s. deviations in bond length and angles are the deviations from ideal values.
[6]Data from phasing programs

two ions were bound to surface exposed His49 (Zn3) and His71 (Zn4). Zn1 was coordinated by a water molecule, Glu217, His220, Asp255, and Asp257 in a trigonal bipyramidal geometry (Fig. 2) and a water molecule, Glu181, Glu217, Asp245, and Asp287 coordinate Zn2 in a octahedral geometry (Fig. 2). Surface bound Zn3 and Zn4 were coordinated by one water molecule and one acetate molecule (Zn3, Fig. 2) or by a histidine residue and three water molecules (Zn4, Fig. 2) in a tetrahedral geometry. In the anomalous difference Fourier map contoured at 5σ, the peak of Zn3 was not shown due to its weak anoma-

Table 2. Data collection, phasing and refinement statistics

Protein name	*Sa*Fur														
Data collection	SAD														
Space group	$P4_3$														
X-ray source	In-house Cu $K\alpha$														
Wavelength (Å)	1.54178														
Oscillation (°)	120	150	180	210	240	270	300	330	360	420	480	540	600	660	720
Unit cell parameters *a, b, c* (Å)	68.924, 68.924, 85.746														
Resolution (Å)[1]	50-2.6														
Completeness (%)[1]	99.8 (100.0)	99.9 (100.0)	99.9 (100.0)	99.9 (100.0)	99.9 (100.0)	99.9 (100.0)	99.9 (100.0)	99.9 (100.0)	99.9 (100.0)	99.9 (100.0)	99.9 (100.0)	99.9 (100.0)	99.9 (100.0)	99.9 (100.0)	99.9 (100.0)
R_{merge} (%)[1,2]	7.2 (40.2)	7.7 (39.8)	8.1 (39.9)	8.1 (40.7)	8.2 (41.7)	8.3 (42.5)	8.2 (42.7)	8.4 (42.8)	8.5 (43.0)	8.5 (43.7)	8.4 (43.8)	8.5 (43.7)	8.5 (44.2)	8.5 (44.2)	8.6 (44.1)
$I/\sigma(I)$[1]	38.7 (5.7)	45.6 (6.6)	50.8 (7.3)	54.2 (7.7)	57.6 (8.2)	61.3 (8.8)	65.1 (9.2)	68.7 (9.7)	72.2 (10.1)	77.5 (10.8)	82.7 (11.7)	87.7 (12.4)	92.1 (12.9)	96.9 (13.4)	100.9 (14.0)
Multiplicity	4.8 (4.7)	6.0 (5.9)	7.2 (7.1)	8.4 (8.1)	9.6 (9.3)	10.9 (10.6)	12.1 (11.7)	13.2 (12.8)	14.4 (14.0)	16.9 (16.5)	19.4 (18.8)	21.8 (21.3)	24.2 (23.5)	26.6 (25.9)	29.0 (28.2)
<*d*″/sig> of outer shell[3]	1.09	1.11	1.09	1.09	1.08	1.10	1.13	1.13	1.13	1.15	1.19	1.20	1.20	1.23	1.25
Phasing statistics															
Success of phasing	Failure	Failure	Failure	Success	Success	Success	Success	Success	Success	Success	Success	Success	Success	Success	Success
No. of Zn sites in initial model from *AutoSol*	6	5	6	5	8	7	8	7	7	7	6	6	7	6	7
Sites occupancies[6]	1.00	1.00	1.00	1.00	0.41-1.00	0.83-1.00	1.00	0.52-1.00	0.94-1.00	0.69-1.00	1.00	1.00	1.00	1.00	0.40-1.00
FOM[6]															
Before DM	0.29	0.28	0.31	0.32	0.36	0.36	0.37	0.37	0.39	0.39	0.38	0.9	0.40	0.41	0.42
After DM	0.80	0.79	0.79	0.80	0.81	0.81	0.81	0.79	0.81	0.81	0.81	0.81	0.81	0.82	0.82
Model-map CC[6]	0.28	0.35	0.38	0.49	0.53	0.55	0.54	0.60	0.53	0.54	0.53	0.55	0.55	0.50	0.51
R_{work}[4](R_{free}) (%)	0.4777/ 0.5310	0.4804/ 0.5085	0.4881/ 0.4953	0.4592/ 0.5015	0.4268/ 0.4884	0.4214/ 0.4586	0.4344/ 0.4737	0.3899/ 0.4361	0.4048/ 0.4422	0.4010/ 0.4259	0.4101/ 0.4467	0.4197/ 0.4458	0.4235/ 0.4733	0.4312/ 0.4741	0.4455/ 0.4706

Refinement statistics	
Resolution range (Å)	26.82-2.6
No. reflections	12264
No. atoms	
Protein	2389
Zinc ion	6
Chloride ion	2
R_{work}[4](R_{free}) (%)	19.15 (23.92)
R.m.s. deviations[5]	
Bonds length (Å)	0.003
Bond Angles (°)	0.756

[1]The number in parentheses is for the outer shell.
[2]$R_{merge} = \Sigma_{hkl}\Sigma_i|I_i(hkl) - \langle I(hkl)\rangle|/\Sigma_{hkl}\Sigma_i I_i(hkl)$, where $I_i(hkl)$ is the intensity of observed reflection *hkl* and $\langle I(hkl)\rangle$ is the mean intensity of symmetry-equivalent reflections
[3]Data from *SHELXC* (Sheldrick, 2010)
[4]$R_{work} = \Sigma\,|F_o-F_c|\,/\,\Sigma\,F_o$
R_{free} was calculated with 5% of the reflections.
[5]R.m.s. deviations in bond length and angles are the deviations from ideal values.
[6]Data from phasing programs

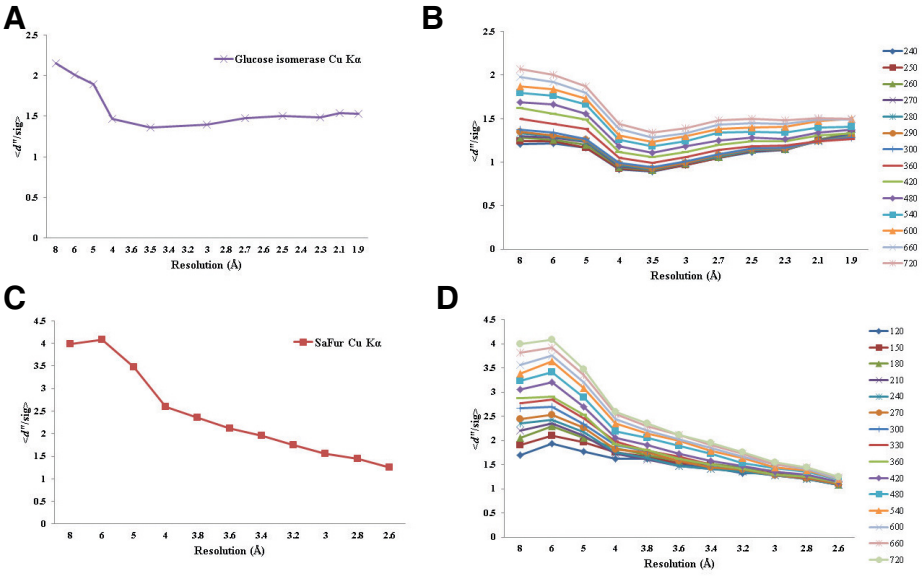

Fig. 1. The <*d*″/sig> plots from SHELXC as a function of resolution. (A) The plot of glucose isomerase 720° oscillation data. (B) The plots of glucose isomerase depending on the multiplicity. (C) The plot of *Sa*Fur 720° oscillation data and (D) The plots of *Sa*Fur depending on the multiplicity.

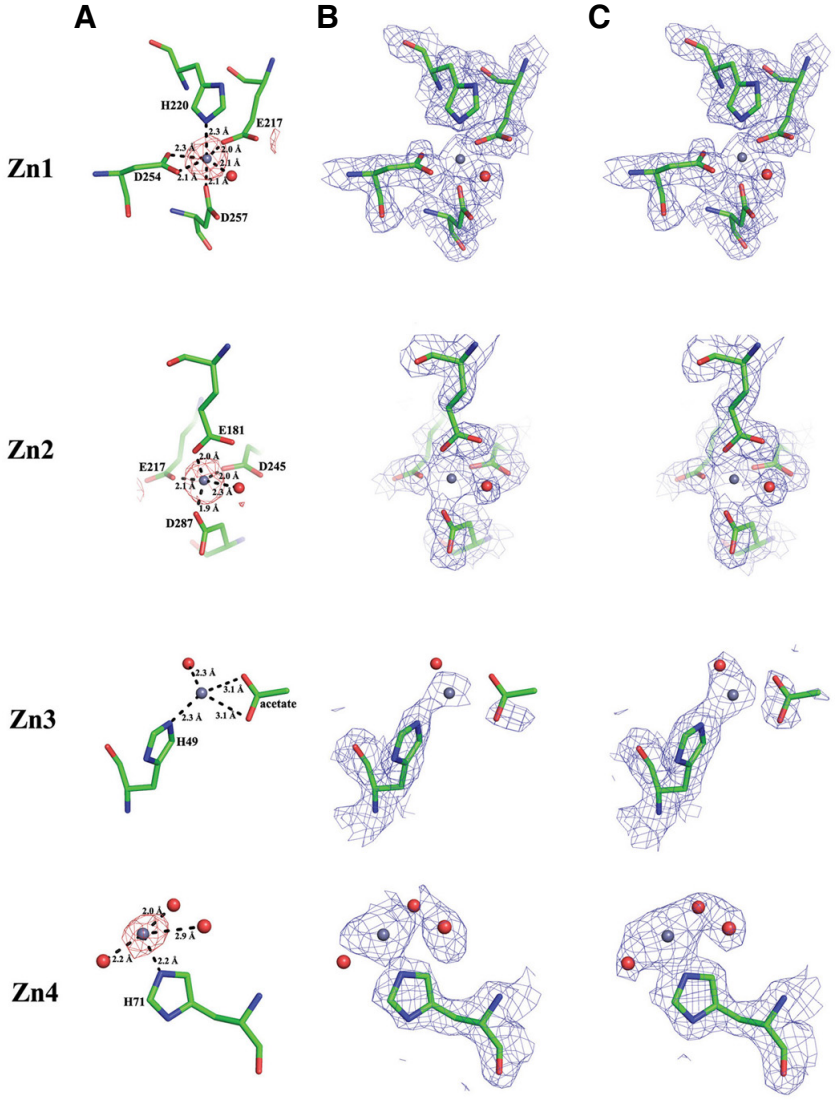

Fig. 2. Anomalous Fourier maps at the 5σ level (A), experimental electron-density maps after density modification (B) and final $2F_o$-F_c maps (C) at the 1σ level superposed onto zinc-binding sites in the final model of glucose isomerase. Zinc ions and water molecules are represented by gray and red spheres, respectively.

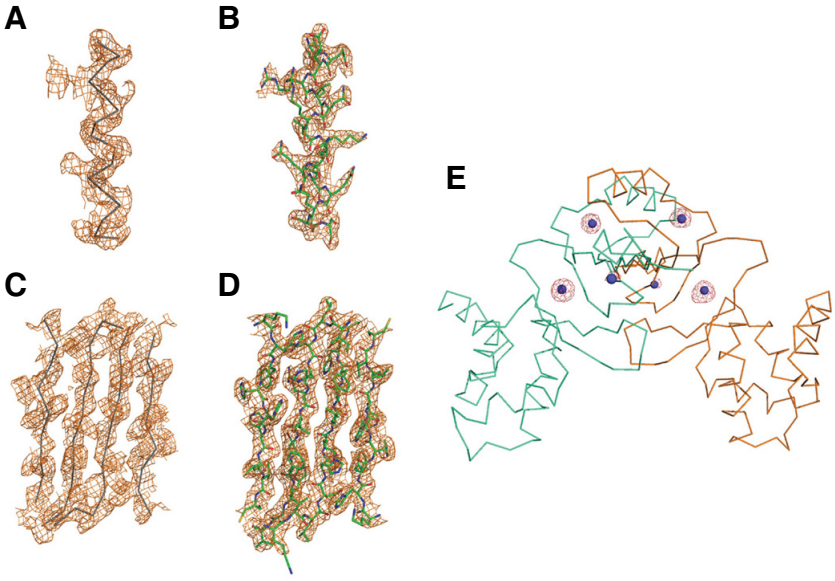

Fig. 3. Representative experimental electron-density maps of α-helix (A) and β-sheet regions (C) with C_α-chain of initial model and final $2F_o$-F_c maps corresponding to (A), (C) at the 1σ level superposed onto the same regions of final model with (B), (D), respectively. Anomalous Fourier map at the 5σ level superposed onto the final *Sa*Fur dimer ribbon model and it clearly shows the six zinc binding sites (E).

lous signal intensity even though the clear electron density that is connected to the $N^{\varepsilon 2}$ atom of His49 was present in both initial and final $2F_o$-F_c maps (Fig. 2).

There is the possibility that Mg^{2+} could be at the Zn1 and Zn2 sites considering the abundance of Mg^{2+} in the crystallization solution. To ensure the existence of zinc ions at the two sites, we compared the thermal *B*-factors because the *B*-factor of a properly determined and refined metal ion should be close to the *B*-factors of its coordinating atoms (Harding, 2004; Zheng et al., 2008). The *B*-factors calculated with zinc ions at the sites (Zn1 = 11.74 Å^2, Zn2 = 11.96 Å^2) were similar to those of the coordinating atoms (Zn1 = 8.81, 8.53, 9.96, 9.66, 10.04 Å^2, Zn2 = 8.47, 8.63, 10.03, 10.31, 11.02, 10.13 Å^2), whereas the *B*-factors of Mg^{2+} located at the two sites were refined to 1 Å^2 displaying a large discrepancy compared with liganding atoms. The spare F_o-F_c electron-density when Mg^{2+} is fitted at the Zn1 and Zn2 sites also supports the assignment of zinc.

In-house SAD phasing generally requires high redundant data to accurately measure the subtle anomalous signal. Therefore, we rescaled the SAD data set of the total 720 frames to evaluate the effect of multiplicity (1-240 to 1-720 with 60° oscillation interval, Table 1). Despite the presence of a reasonable anomalous signal (Fig. 1B), the low multiplicity data set of 1-240 frames was not sufficient to find zinc substructure solutions using *AutoSol*. In this case, a multiplicity of ~9 seems to be the minimum data required for successful Zn-SAD phasing. To date, most of the successful S-SAD cases required a minimum multiplicity of > 10 and there were even cases with a multiplicity of > 50 (Doutch et al., 2012). Therefore, in-house Zn-SAD can be a good alternative to S-SAD in the perspective of the radiation damage problems.

A real case: structure determination of *Sa*Fur using in-house Zn-SAD

*Sa*Fur is a homodimeric protein and each monomer consists of 149 amino acids. *Sa*Fur is an iron-sensing transcriptional regulator involved in intracellular iron homeostasis and belongs to the ferric uptake regulator (Fur) family which includes sensors of Fe (Fur), Zn (Zur) and Ni (Nur) (Lee and Helmann, 2007). Fur family proteins contain metal sites and the binding of metal ions modulates their DNA-binding activity. Despite the fact that Fur proteins are Fe-sensing proteins, the crystal structures of *Pseudomonas aeruginosa* Fur (*Pa*Fur) (Pohl et al., 2003), *Vibrio cholera* Fur (*Vc*Fur) (Sheikh and Taylor, 2009), *Helicobacter pylori* Fur (*Hp*Fur) (Dian et al., 2011), and *Campylorbacter jejuni* Fur (*Cj*Fur) (Butcher et al., 2012) revealed that the metal sites of all these four proteins are occupied by zinc atoms. Except for *Vc*Fur structure, other Fur structures were determined using zinc anomalous scattering. Since our trials of molecular replacement to solve the structure of *Sa*Fur resulted in failure, we thought that *Sa*Fur was an optimal real case for the in-house Zn-SAD phasing. We collected a 2.6 Å resolution SAD data set (Table 2) from a crystal that was cooled in a cryostream at 100 K after briefly being immersed in a cryoprotectant solution consisting of 30% (v/v) 1,2-propanediol, 0.1 M HEPES pH 7.5, 20% (v/v) PEG 400. The crystal of *Sa*Fur belonged to the tetragonal space group, $P4_3$, with unit-cell parameters a = b = 68.804, c = 85.526 Å. There are two molecules in the asymmetric unit, giving a Matthews coefficient (V_M) of 2.94 Å^3 Da^{-1} and a calculated solvent content of 58.12% (Matthews, 1968).

According to the plot of <*d*″/sig> *versus* resolution (Fig. 1C), the zinc anomalous signal was high over the entire resolution range. A total of six zinc ions, with occupancies of 0.08-1.00, were identified in the asymmetric unit and the resulting phasing set, characterized by an FOM of 0.42, yielded an interpretable electron-density map (Figs. 3A and 3C) leading to an auto-built model consisting of 194 residues among the total 298 amino acids with R_{work}/R_{free} of 0.4455/0.4706. Further model building was performed manually using the program *COOT* and the iterative rounds of refinement were performed using the program *REFMAC5*. The final model with R_{work}/R_{free} of 0.1915/0.2392 clearly shows that the dimeric closed form of *Sa*Fur and DNA binding α4 helices are positioned toward the putative DNA-binding site. An anomalous difference Fourier map showed six significant peaks > 5σ (Fig. 3E). Their distinctive intensities of anomalous signals are compatible with the fact that three metal sites in the Fur family proteins (one structural metal site, two regulatory metal sites) have a different affinity to metal ions (An et al., 2009; Dian et al., 2011; Lucarelli et al., 2007; Shin et al., 2011). The metal sites of *Sa*Fur were occupied by zinc atoms,

as are in the cases of Fur proteins whose structures are available, even though 10 mM EDTA was treated during purification in order to obtain zinc-free proteins. It is noteworthy that the purified *Sa*Fur can bind to its target DNA sequence (data not shown). The detailed structural features of *Sa*Fur will be published elsewhere.

In contrast to the case of glucose isomerase, no sulfur atoms of methionines or cysteines were found in substructure solutions. To the best of our knowledge, this is the first report describing successful in-house Zn-SAD phasing experiments. The successful in-house Zn-SAD phasing of *Sa*Fur, solely with a zinc anomalous signal from the modest 2.6 Å resolution data collected using Cu $K\alpha$ X-ray radiation, expands the limit of the application range of in-house Zn-SAD phasing to protein crystals that have no ordered native sulfur atoms.

The SAD data set of total 720 frames was rescaled to see the effect of multiplicity (1-120 to 1-360 with 30° oscillation interval, 1-360 to 1-720 with 60° oscillation interval, Table 2). Despite the presence of a reasonable anomalous signal (Fig. 1D), the low multiplicity data set 1-120 to 1-180 were not sufficient to give interpretable experimental electron-density maps with *AutoSol*. In this case, a multiplicity of ~8.4 was defined as the minimum data required for successful Zn-SAD phasing, comparable to the case of glucose isomerase.

CONCLUSION

We demonstrated that protein crystals containing multiple zinc ions are suitable for Zn-SAD phasing using in-house Cu $K\alpha$ X-ray source. We also expect successful Zn-SAD phasing using in-house Cd $K\alpha$ radiation (λ = 2.1 Å) due to the higher f'' value of zinc atoms (f'' = 1.18 e^-) at Cd $K\alpha$ edge than at Cu $K\alpha$ edge (f'' = 0.98 e^-). Until now, there are about 8,000 structures (= ~10%) with zinc ions as ligands in the PDB, and these numbers are the highest among possible anomalous scatterers for experimental phasing. Furthermore, in our previous study, we have shown that Zn-SAD phasing can be extended to the protein crystals with no intrinsic zinc binding sites (Cha et al., 2012). Thus, considering the abundance of zinc-binding proteins in nature, the easy zinc derivatization of the protein surface (Cha et al., 2012), our success in in-house Zn-SAD phasing with the modest 2.6 Å resolution SAD data indicate that in-house Zn-SAD phasing can be widely applicable to structure determination without synchrotron access.

ACKNOWLEDGMENTS

This work was supported by the National Research Foundation of Korea Grant 2012005978, the CAP through Korea Research Council of Fundamental Science Technology (KRCF), Korea Institute of Science and Technology (KIST), & Korea Institute of Ocean Science and Technology (KIOST), the Marine and Extreme Genome Research Center program and the Development of Biohydrogen Production Technology Using Hyperthermophilic Archaea program of MLTM, and the KIOST in-house NSC program. The work performed at Hanyang University was supported by the Korea Research Foundation Grant funded by the Korean Goverment (KRF-2008-313-C00774) and by Mid-career Researcher Program through NRF grant funded by the [The Ministry of Education, Science and Technology (MEST)] (NRF-2012-0005445).

REFERENCES

Adams, P.D., Afonine, P.V., Bunkoczi, G., Chen, V.B., Davis, I.W., Echols, N., Headd, J.J., Hung, L.W., Kapral, G.J., Grosse-Kunstleve, R.W., et al. (2010). PHENIX: a comprehensive Python-based system for macromolecular structure solution. Acta Crystallogr. D Biol. Crystallogr. *66*, 213-221.

An, Y.J., Ahn, B.E., Han, A.R., Kim, H.M., Chung, K.M., Shin, J.H., Cho, Y.B., Roe, J.H., and Cha, S.S. (2009). Structural basis for the specialization of Nur, a nickel-specific Fur homolog, in metal sensing and DNA recognition. Nucleic Acids Res. *37*, 3442-3451.

Andreini, C., Banci, L., Bertini, I., and Rosato, A. (2006). Zinc through the three domains of life. J. Proteome Res. *5*, 3173-3178.

Blundell, T.L., and Johnson, L.N. (1976). Protein Crystallography (Academic Press, New York).

Boggon, T.J., and Shapiro, L. (2000). Screening for phasing atoms in protein crystallography. Structure *8*, R143-149.

Brunger, A.T., Adams, P.D., Clore, G.M., DeLano, W.L., Gros, P., Grosse-Kunstleve, R.W., Jiang, J.S., Kuszewski, J., Nilges, M., Pannu, N.S., et al. (1998). Crystallography & NMR system: a new software suite for macromolecular structure determination. Acta Crystallogr. D Biol. Crystallogr. *54*, 905-921.

Butcher, J., Sarvan, S., Brunzelle, J.S., Couture, J.F., and Stintzi, A. (2012). Structure and regulon of Campylobacter jejuni ferric uptake regulator Fur define apo-Fur regulation. Proc. Natl. Acad. Sci. USA *109*, 10047-10052.

Cha, S.S., An, Y.J., Jeong, C.S., Kim, M.K., Lee, S.G., Lee, K.H., and Oh, B.H. (2012). Experimental phasing using zinc anomalous scattering. Acta Crystallogr. D Biol. Crystallogr. *68*, 1253-1258.

Chayen, N.E., Cianci, M., Olczak, A., Raftery, J., Rizkallah, P.J., Zagalsky, P.F., and Helliwell, J.R. (2000). Apocrustacyanin A1 from the lobster carotenoprotein alpha-crustacyanin: crystallization and initial X-ray analysis involving softer X-rays. Acta Crystallogr. D Biol. Crystallogr. *56*, 1064-1066.

Dauter, Z., and Adamiak, D.A. (2001). Anomalous signal of phosphorus used for phasing DNA oligomer: importance of data redundancy. Acta Crystallogr. D Biol. Crystallogr. *57*, 990-995.

Dauter, Z., Dauter, M., de La Fortelle, E., Bricogne, G., and Sheldrick, G.M. (1999). Can anomalous signal of sulfur become a tool for solving protein crystal structures? J. Mol. Biol. *289*, 83-92.

Dauter, Z., Dauter, M., and Dodson, E. (2002). Jolly SAD. Acta Crystallogr. D Biol. Crystallogr. *58*, 494-506.

Debreczeni, J.E., Bunkoczi, G., Girmann, B., and Sheldrick, G.M. (2003a). In-house phase determination of the lima bean trypsin inhibitor: a low-resolution sulfur-SAD case. Acta Crystallogr. D Biol. Crystallogr. *59*, 393-395.

Debreczeni, J.E., Bunkoczi, G., Ma, Q., Blaser, H., and Sheldrick, G.M. (2003b). In-house measurement of the sulfur anomalous signal and its use for phasing. Acta Crystallogr. D Biol. Crystallogr. *59*, 688-696.

Debreczeni, J.E., Girmann, B., Zeeck, A., Kratzner, R., and Sheldrick, G.M. (2003c). Structure of viscotoxin A3: disulfide location from weak SAD data. Acta Crystallogr. D Biol. Crystallogr. *59*, 2125-2132.

Dian, C., Vitale, S., Leonard, G.A., Bahlawane, C., Fauquant, C., Leduc, D., Muller, C., de Reuse, H., Michaud-Soret, I., and Terradot, L. (2011). The structure of the Helicobacter pylori ferric uptake regulator Fur reveals three functional metal binding sites. Mol. Microbiol. *79*, 1260-1275.

Doutch, J., Hough, M.A., Hasnain, S.S., and Strange, R.W. (2012). Challenges of sulfur SAD phasing as a routine method in macromolecular crystallography. J. Synchrotron. Radiat. *19*, 19-29.

Emsley, P., Lohkamp, B., Scott, W.G., and Cowtan, K. (2010). Features and development of Coot. Acta Crystallogr. D Biol. Crystallogr. *66*, 486-501.

Evans, G., and Bricogne, G. (2003). Triiodide derivatization in protein crystallography. Acta Crystallogr. D Biol. Crystallogr. *59*, 1923-1929.

Grosse-Kunstleve, R.W., and Adams, P.D. (2003). Substructure search procedures for macromolecular structures. Acta Crystallogr. D Biol. Crystallogr. *59*, 1966-1973.

Harding, M.M. (2004). The architecture of metal coordination groups in proteins. Acta Crystallogr. D Biol. Crystallogr. *60*, 849-859.

Hendrickson, W.A. (1991). Determination of macromolecular structures from anomalous diffraction of synchrotron radiation. Science *254*, 51-58.

Hendrickson, W.A., and Teeter, M.M. (1981). Structure of the hydrophobic protein crambin determined directly from the anomalous scattering of sulphur. Nature *290*, 107 -113.

Hendrickson, W.A., Horton, J.R., and LeMaster, D.M. (1990). Sele-

nomethionyl proteins produced for analysis by multiwavelength anomalous diffraction (MAD): a vehicle for direct determination of three-dimensional structure. EMBO J. *9*, 1665-1672.
Islam, S.A., Carvin, D., Sternberg, M.J., and Blundell, T.L. (1998). HAD, a data bank of heavy-atom binding sites in protein crystals: a resource for use in multiple isomorphous replacement and anomalous scattering. Acta Crystallogr. D Biol. Crystallogr. *54*, 1199-1206.
Lee, J.W., and Helmann, J.D. (2007). Functional specialization within the Fur family of metalloregulators. Biometals *20*, 485-499.
Lemke, C.T., Smith, G.D., and Howell, P.L. (2002). S-SAD, Se-SAD and S/Se-SIRAS using Cu Kalpha radiation: why wait for synchrotron time? Acta Crystallogr. D Biol. Crystallogr. *58*, 2096-2101.
Leonard, G.A., Sainz, G., de Backer, M.M., and McSweeney, S. (2005). Automatic structure determination based on the single-wavelength anomalous diffraction technique away from an absorption edge. Acta Crystallogr. D Biol. Crystallogr. *61*, 388-396.
Lucarelli, D., Russo, S., Garman, E., Milano, A., Meyer-Klaucke, W., and Pohl, E. (2007). Crystal structure and function of the zinc uptake regulator FurB from *Mycobacterium tuberculosis*. J. Biol. Chem. *282*, 9914-9922.
Matthews, B.W. (1968). Solvent content of protein crystals. J. Mol. Biol. *33*, 491-497.
McCoy, A.J., Grosse-Kunstleve, R.W., Adams, P.D., Winn, M.D., Storoni, L.C., and Read, R.J. (2007). Phaser crystallographic software. J. Appl. Crystallogr. *40*, 658-674.
Mueller-Dieckmann, C., Polentarutti, M., Djinovic Carugo, K., Panjikar, S., Tucker, P.A., and Weiss, M.S. (2004). On the routine use of soft X-rays in macromolecular crystallography. Part II. Data-collection wavelength and scaling models. Acta Crystallogr. D Biol. Crystallogr. *60*, 28-38.
Mueller-Dieckmann, C., Panjikar, S., Tucker, P.A., and Weiss, M.S. (2005). On the routine use of soft X-rays in macromolecular crystallography. Part III. The optimal data-collection wavelength. Acta Crystallogr. D Biol. Crystallogr. *61*, 1263-1272.
Mueller-Dieckmann, C., Panjikar, S., Schmidt, A., Mueller, S., Kuper, J., Geerlof, A., Wilmanns, M., Singh, R.K., Tucker, P.A., and Weiss, M.S. (2007). On the routine use of soft X-rays in macromolecular crystallography. Part IV. Efficient determination of anomalous substructures in biomacromolecules using longer X-ray wavelengths. Acta Crystallogr. D Biol. Crystallogr. *63*, 366-380.
Murshudov, G.N., Skubak, P., Lebedev, A.A., Pannu, N.S., Steiner, R.A., Nicholls, R.A., Winn, M.D., Long, F., and Vagin, A.A. (2011). REFMAC5 for the refinement of macromolecular crystal structures. Acta Crystallogr. D Biol. Crystallogr. *67*, 355-367.
Olczak, A., Cianci, M., Hao, Q., Rizkallah, P.J., Raftery, J., and Helliwell, J.R. (2003). S-SWAT (softer single-wavelength anomalous technique): potential in high-throughput protein crystallography. Acta Crystallogr. A *59*, 327-334.
Olsen, J.G., Flensburg, C., Olsen, O., Bricogne, G., and Henriksen, A. (2004). Solving the structure of the bubble protein using the anomalous sulfur signal from single-crystal in-house Cu Kalpha diffraction data only. Acta Crystallogr. D Biol. Crystallogr. *60*, 250-255.
Otwinowski, Z., and Minor, W. (1997). Processing of X-ray diffraction data collected in oscillation mode. Method Enzymol. *276*, 307-326.
Pal, A., Debreczeni, J.E., Sevvana, M., Gruene, T., Kahle, B., Zeeck, A., and Sheldrick, G.M. (2008). Structures of viscotoxins A1 and B2 from European mistletoe solved using native data alone. Acta Crystallogr. D Biol. Crystallogr. *64*, 985-992.
Petsko, G.A. (1985). Preparation of isomorphous heavy-atom derivatives. Methods Enzymol. *114*, 147-156.
Pohl, E., Haller, J.C., Mijovilovich, A., Meyer-Klaucke, W., Garman, E., and Vasil, M.L. (2003). Architecture of a protein central to iron homeostasis: crystal structure and spectroscopic analysis of the ferric uptake regulator. Mol. Microbiol. *47*, 903-915.
Ramagopal, U.A., Dauter, M., and Dauter, Z. (2003a). Phasing on anomalous signal of sulfurs: what is the limit? Acta Crystallogr. D Biol. Crystallogr. *59*, 1020-1027.
Ramagopal, U.A., Dauter, M., and Dauter, Z. (2003b). SAD manganese in two crystal forms of glucose isomerase. Acta Crystallogr. D Biol. Crystallogr. *59*, 868-875.
Roeser, D., Dickmanns, A., Gasow, K., and Rudolph, M.G. (2005). De novo calcium/sulfur SAD phasing of the human formylglycine-generating enzyme using in-house data. Acta Crystallogr. D Biol. Crystallogr. *61*, 1057-1066.
Rould, M.A. (1997). Screening for heavy-atom derivatives and obtaining accurate isomorphous differences. Method Enzymol. *276*, 461-472.
Sarma, G.N., and Karplus, P.A. (2006). In-house sulfur SAD phasing: a case study of the effects of data quality and resolution cutoffs. Acta Crystallogr. D Biol. Crystallogr. *62*, 707-716.
Sheikh, M.A., and Taylor, G.L. (2009). Crystal structure of the Vibrio cholerae ferric uptake regulator (Fur) reveals insights into metal co-ordination. Mol. Microbiol. *72*, 1208-1220.
Sheldrick, G.M. (2010). Experimental phasing with SHELXC/D/E: combining chain tracing with density modification. Acta Crystallogr. D Biol. Crystallogr. *66*, 479-485.
Shin, J.H., Jung, H.J., An, Y.J., Cho, Y.B., Cha, S.S., and Roe, J.H. (2011). Graded expression of zinc-responsive genes through two regulatory zinc-binding sites in Zur. Proc. Natl. Acad. Sci. USA *108*, 5045-5050.
Stevenson, C.E., Tanner, A., Bowater, L., Bornemann, S., and Lawson, D.M. (2004). SAD at home: solving the structure of oxalate decarboxylase with the anomalous signal from manganese using X-ray data collected on a home source. Acta Crystallogr. D Biol. Crystallogr. *60*, 2403-2406.
Terwilliger, T.C. (2002). Automated structure solution, density modification and model building. Acta Crystallogr. D Biol. Crystallogr. *58*, 1937-1940.
Terwilliger, T.C., Adams, P.D., Read, R.J., McCoy, A.J., Moriarty, N.W., Grosse-Kunstleve, R.W., Afonine, P.V., Zwart, P.H., and Hung, L.W. (2009). Decision-making in structure solution using Bayesian estimates of map quality: the PHENIX AutoSol wizard. Acta Crystallogr. D Biol. Crystallogr. *65*, 582-601.
Vennila, K.N., and Velmurugan, D. (2011). In-house SAD phasing with surface-bound cerium ions. Acta Crystallogr. Sect. F Struct. Biol. Cryst. Commun. *67*, 1662-1665.
Wang, B.C. (1985). Resolution of phase ambiguity in macromolecular crystallography. Methods Enzymol. *115*, 90-112.
Weiss, M.S., Sicker, T., Djinovic-Carugo, K., and Hilgenfeld, R. (2001). On the routine use of soft X-rays in macromolecular crystallography. Acta Crystallogr. D Biol. Crystallogr. *57*, 689-695.
Yang, C., and Pflugrath, J.W. (2001). Applications of anomalous scattering from S atoms for improved phasing of protein diffraction data collected at Cu Kalpha wavelength. Acta Crystallogr. D Biol. Crystallogr. *57*, 1480-1490.
Yogavel, M., Gill, J., Mishra, P.C., and Sharma, A. (2007). SAD phasing of a structure based on cocrystallized iodides using an in-house Cu Kalpha X-ray source: effects of data redundancy and completeness on structure solution. Acta Crystallogr. D Biol. Crystallogr. *63*, 931-934.
Yogavel, M., Gill, J., and Sharma, A. (2009). Iodide-SAD, SIR and SIRAS phasing for structure solution of a nucleosome assembly protein. Acta Crystallogr. D Biol. Crystallogr. *65*, 618-622.
Yogavel, M., Khan, S., Bhatt, T.K., and Sharma, A. (2010a). Structure of D-tyrosyl-tRNATyr deacylase using home-source Cu Kalpha and moderate-quality iodide-SAD data: structural polymorphism and HEPES-bound enzyme states. Acta Crystallogr. D Biol. Crystallogr. *66*, 584-592.
Yogavel, M., Nithya, N., Suzuki, A., Sugiyama, Y., Yamane, T., Velmurugan, D., and Sharma, A. (2010b). Structural analysis of actinidin and a comparison of cadmium and sulfur anomalous signals from actinidin crystals measured using in-house copper- and chromium-anode X-ray sources. Acta Crystallogr. D Biol. Crystallogr. *66*, 1323-1333.
Zheng, H., Chruszcz, M., Lasota, P., Lebioda, L., and Minor, W. (2008). Data mining of metal ion environments present in protein structures. J. Inorg. Biochem. *102*, 1765-1776.